Hindawi Publishing Corporation
Journal of Nanomaterials
Volume 2015, Article ID 361957, 5 pages
http://dx.doi.org/10.1155/2015/361957

Research Article

Multicolor Emission Tuning and Red/Green Ratio Enhancement of Yb^{3+}/Er^{3+} Codoped $KGdF_4$ Upconversion Nanoparticles

Xionger Qiu and Tiejun Lin

Department of Electrical Engineering, Shaoyang University, Shaoyang, Hunan 422000, China

Correspondence should be addressed to Xionger Qiu; qiujiaqi_0124@163.com

Received 28 January 2015; Accepted 2 March 2015

Academic Editor: Qilin Dai

Herein, a series of $KGdF_4:Yb^{3+}/Er^{3+}$ upconversion nanoparticles (UCNPs) were synthesized through a one-pot hydrothermal method using polyethylene glycol (PEG) as capping ligands. The phase and microstructure studies show all these as-prepared UCNPs are pure cubic phase and uniformed nanoparticle shape by changing the doped Yb^{3+} concentration from 18% to 98%. The as-prepared UCNPs can realize the multicolor emissions from yellow to red and the red-to-green (R/G) ratio can be enhanced from 2.05 to 8.35 when Yb^{3+} varies from 18% to 98%. In addition, the proposed upconversion (UC) mechanisms of these PEGylated UCNPs are investigated in detail. The realization of multicolor tuning and enhanced R/G ratio by only increasing the doping concentration of Yb^{3+} ions in $KGdF_4$ host indicates that the PEGylated $KGdF_4:Yb^{3+}/Er^{3+}$ UCNPs can find their application on lighting devices, anticounterfeit technology, and even bioimaging field.

1. Introduction

In recent years, lanthanides- (Ln-) doped UCNPs have triggered intense research interest and have been widely applied in lighting devices, magnets, anticounterfeit technology, and biomedical field [1–5]. This is due to the fact that their optical, magnetic, electronic, and chemical nature arises from the 4f shell of Ln ions [6–8]. Besides, Ln-doped UCNPs exhibit large antistocks effects, which can convert a longer wavelength light like near-infrared (NIR) to shorter wavelength luminescence (ultraviolet, visible light, and NIR). Among all the well-developed UCNPs, sodium rare-earth fluorides ($NaREF_4$), such as $NaYF_4$, $NaLuF_4$, and $NaGdF_4$, are considered as promising and the most efficient host matrix owing to their normally low photon energy, which can decrease the nonradiative radiation probability and increase the UC emission and quantum yield [9–11]. Boyer et al. [12] have reported that Yb^{3+}/Er^{3+} and Yb^{3+}/Tm^{3+} codoped $NaYF_4$ colloidal UCNPs as the material with high upconversion efficiency. Wang et al. [13] have shown that $NaYF_4$ nanocrystals can simultaneously realize size/phase and UC emission color tuning by doping trivalent Ln ions at defined concentrations. Recently, Tian et al. [14] and Zeng et al. [15] have demonstrated Mn^{2+} doping methods for multicolor tuning and enhanced red UC emission in $NaREF_4$ systems with fixing the doped Yb^{3+} and Er^{3+} concentration. Nevertheless, how to achieve multicolor UC emission and enhanced red emission by only changing the doped Yb^{3+} concentration is still a huge challenge because Yb^{3+}/Er^{3+} codoped UCNPs present green UC emission in general. Recently, Chen et al. [16] have reported that UC NIR emission centered at 800 nm can be enhanced in Yb^{3+}/Tm^{3+} codoped $NaYF_4$ UCNPs along with the increase of Yb^{3+} concentration. This finding inspires us to achieve UC emission color tuning from green to red and to enhance red luminescence in Yb^{3+}/Er^{3+} codoped UCNPs.

Apart from the well-established $NaREF_4$ UCNPs, $KREF_4$ can also act as effect and ideal UC host lattice. For instance, Wong et al. [17] have synthesized small sized Yb^{3+}/Er^{3+} codoped $KGdF_4$ UCNPs via one-pot solvothermal process utilizing branched polyethyleneimine and 6-aminocaproic acid as capping ligands. However, the authors' emphasis has not focused on multicolor tuning and red emission enhancement but the green emission and paramagnetic nature of

these $KGdF_4$:Yb^{3+}/Er^{3+} UCNPs. Importantly, enhanced red emission, considered as "optical window" for live beings, is beneficial to bioimaging for deep tissue penetration. In addition, in spite of the perfect UC host, Gd^{3+}-based nanomaterials can also act as promising T_1-weighted contrast agents for magnetic resonance imaging [9]. However, there are few literatures, up to now, concentrated on $KGdF_4$-hosted UCNPs. Therefore, it is of significance to develop multifunctional Yb^{3+}/Er^{3+} codoped $KGdF_4$ UCNPs using a simple method for emission color tuning and enhanced red emission.

In this work, a series of $KGdF_4$:Yb^{3+}/Er^{3+} UCNPs were fabricated by a one-pot hydrothermal method using PEG as capping ligands. The phase compositions and microstructure of these as-prepared products were characterized by X-ray diffraction (XRD) and field-emission scanning electron microscope (FE-SEM), respectively. The UC properties of these UCNPs were detected using emission spectra and the UC emission mechanisms were analyzed in detail. As excepted, multicolor tuning and enhanced red UC emission were achieved by only tuning the doped Yb^{3+} concentration in the host, which indicated that these as-prepared $KGdF_4$:Yb^{3+}/Er^{3+} UCNPs could expand their application from optics to biomedicine.

2. Experimental Section

2.1. Materials and Regents. $RE(NO_3)_3{\cdot}6H_2O$ (RE = Gd^{3+}, Yb^{3+}, and Er^{3+}, 99.99%) were purchased from Sigma-Aldrich. Ethylene glycol (EG), PEG, KF, and other reagents were purchased from Sinopharm Chemical Reagent Co., China. All of these chemicals were used as received without further purification.

2.2. One-Pot Method for Fabrication of $KGdF_4$:Yb^{3+}/Er^{3+} UCNPs. $KGdF_4$:x%Yb^{3+}/2%Er^{3+} (x = 18, 38, 58, 78, and 98) UCNPs were synthesized through a simple one-pot hydrothermal method using PEG as a surface modifier [10]. In a typical process, 1.0 g of PEG was dissolved into 15 mL of EG solution for the formation of aqueous solution. And then, a total amount (1 mmol) of $RE(NO_3)_3$ water solutions with as-designed molar ratio was added. After 10 min agitation, 6 mL of KF aqueous solution (1 mM) was added into the former mixture. After another 30 min agitation, the mixture was poured in a 50 mL Teflon-lined stainless steel autoclave. The system was sealed and kept at 200°C for 24 h. After reaction, the system was cooled to room temperature and the product was washed with absolute ethyl alcohol and deionized water and dried at 60°C for 24 h.

2.3. Characterizations. XRD analysis was measured by a D/max-γA System X-ray diffractometer at 40 kV and 250 mA with Cu-Kα radiation (λ = 1.54056 Å). Morphologies of these UCNPs were characterized by FE-SEM (FEI NanoSEM 450). UC photoluminescence spectra of these UCNPs were recorded by a Zolix analytical instrument (fluoroSENS 9000A) equipped with a 980 nm laser.

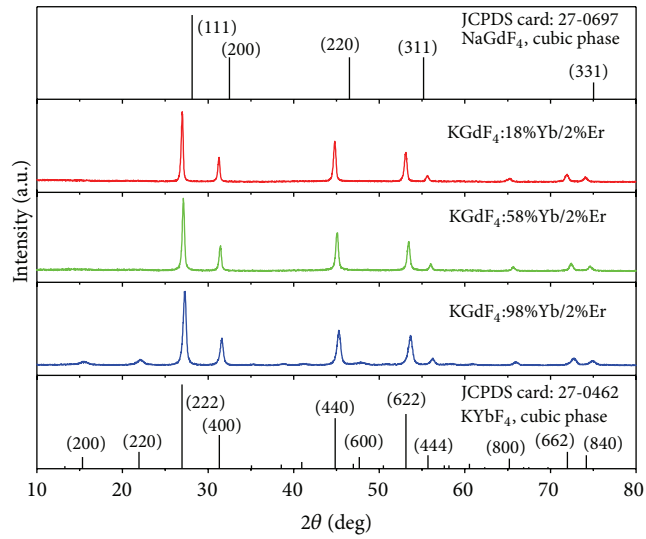

Figure 1: XRD patterns of $KGdF_4$:18%Yb^{3+}/2%Er^{3+}, $KGdF_4$:58%Yb^{3+}/2%Er^{3+}, $KGdF_4$:98%Yb^{3+}/2%Er^{3+} UCNPs, and standard JCPDS Card of cubic phase $NaGdF_4$ and $KYbF_4$.

3. Results and Discussion

Crystal phases and compositions of these as-prepared $KGdF_4$:Yb^{3+}/Er^{3+} UCNPs were synthesized by a simple one-pot hydrothermal process utilizing PEG as capping ligands. These UCNPs were recorded by powder XRD patterns. As presented by the red line in Figure 1, the measured XRD pattern of the PEGylated $KGdF_4$:18%Yb^{3+}/2%Er^{3+} UCNPs is in agreement with that reported in previous literatures [16], which is similar to that of the cubic phase $NaGdF_4$ (JCPDS Card: 27-0697) and space group *Fm3m*. It therefore can be seen that the $KGdF_4$:18%Yb^{3+}/2%Er^{3+} UCNPs crystallize in the fluorite structure known for cubic phase $NaGdF_4$. When the doped Yb^{3+} concentration increases by 58%, the diffraction peaks shift towards high angel sides owing to the replacement of Gd^{3+} (1.193 Å) by relatively smaller Yb^{3+} ions (1.125 Å) in the host [17]. After the total substitution of Gd^{3+} through Yb^{3+}, the UCNPs show the pure cubic $KYbF_4$ phase (JCPDS Card: 27-0462). As observed, all these as-prepared UCNPs are of pure and single cubic phase.

To further study the morphology of these PEGylated UCNPs, FE-SEM images were carried out. As shown in Figures 2(a)–2(e), all these as-prepared PEGylated UCNPs are uniformed nanoparticle shape and the high doping has not changed the crystal structures and morphology of the host materials. The average diameter of these UCNPs is measured to 86.7, 64.8, 60.8, 46.6, and 43.1 nm while the doping ions of Yb^{3+} vary from 18% to 98% based on FE-SEM images. In addition, the EDS of $KGdF_4$:18%Yb^{3+}/2%Er^{3+} UCNPs (Figure 2(f)) shows the major elements composition of K, Gd, and Yb. The detected C and Si come from the silicon pellet of FE-SEM. In addition, the absence signal of Er element is due to the low doping concentration and the accuracy of the detector. Figure 2(g) shows the EDS of

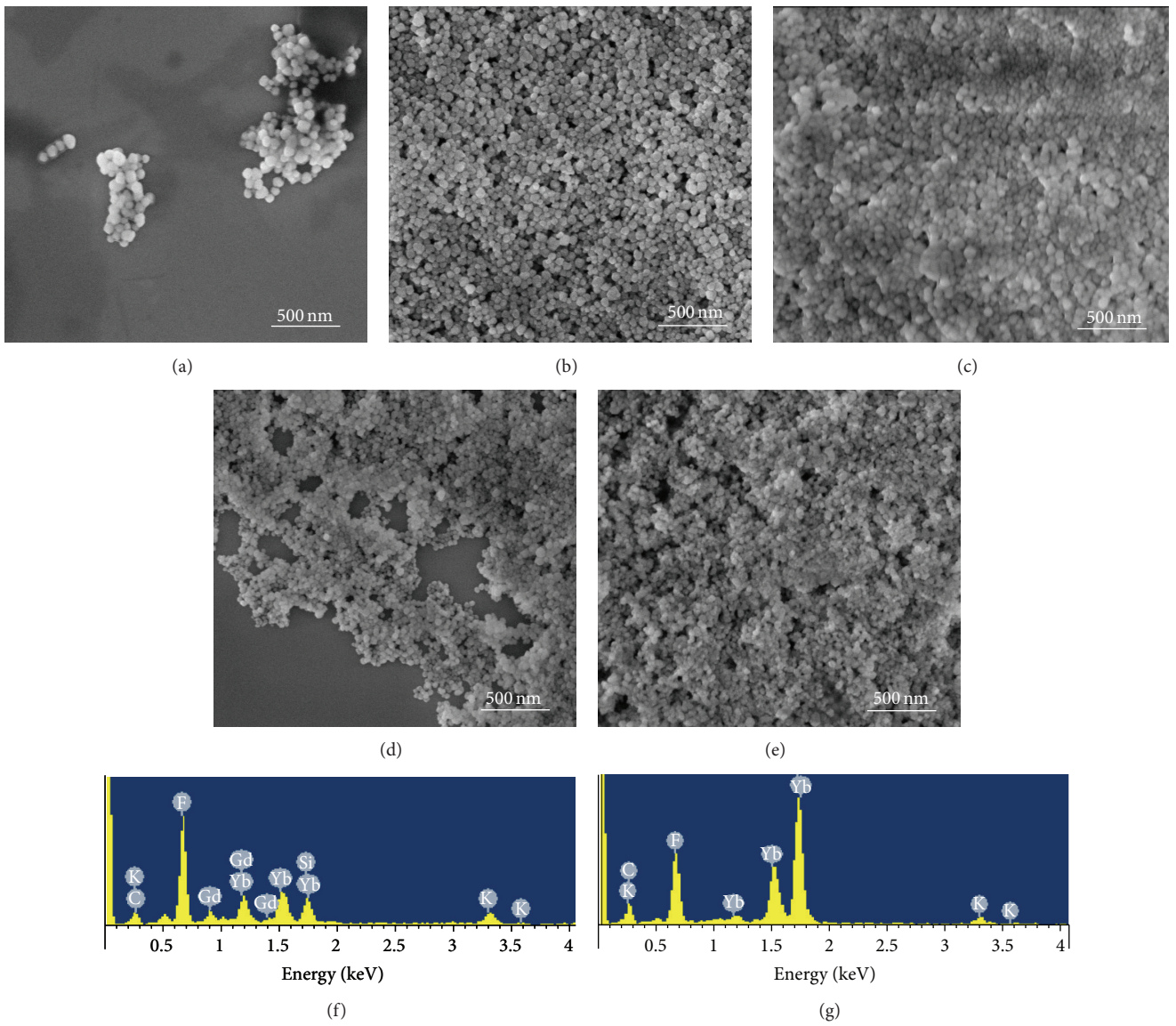

FIGURE 2: FE-SEM images of $KGdF_4$:Yb^{3+}/Er^{3+} UCNPs with doping different Yb^{3+} ions: (a) 18%, (b) 38%, (c) 58%, (d) 78%, and (e) 98%; the EDS of (f) $KGdF_4$:18%Yb^{3+}/2%Er^{3+} and (g) $KGdF_4$:98%Yb^{3+}/2%Er^{3+} UCNPs.

$KGdF_4$:98%Yb^{3+}/2%Er^{3+} UCNPs, indicating the absolute substitution of Gd by Yb elements in the nanocrystals.

Figure 3 gives the UC emission spectra of $KGdF_4$:x%Yb^{3+}/2%Er^{3+} (x = 18, 38, 58, 78, and 98) UCNPs with different doping concentration of Yb^{3+}. The emission bands can be attributed to the $^2H_{11/2} \rightarrow {}^4I_{15/2}$, $^4S_{3/2} \rightarrow {}^4I_{15/2}$, and $^4F_{9/2} \rightarrow {}^4I_{15/2}$ transitions of Er^{3+}, respectively [18, 19]. As observed in Figure 3, $KGdF_4$:Yb^{3+}/Er^{3+} UCNPs present the strong green and red emission when doping 18% Yb^{3+}. However, the green emission has been inhibited and the R/G ratio (Figure 4) can be promoted from 2.05 to 2.28, 3.12, 3.48, and finally 8.35 by ranging from the doping concentration of Yb^{3+} from 18% to 98%. The corresponding CIE chromaticity of $KGdF_4$:x%Yb^{3+}/2%Er^{3+} (x = 18, 38, 58, 78, and 98) UCNPs is shown in Figure 5. The output emission colors tune obviously from the yellow region to the red region with the increase of the doped Yb^{3+} concentration owing to the intensities variation of the green and red emissions.

To further understand the UC emission properties of the PEGylated $KGdF_4$:Yb^{3+}/Er^{3+} UCNPs by tuning the doped Yb^{3+} concentration, the proposed UC mechanisms should be investigated in detail. As illustrated in Figure 6, the first energy transfer from Yb^{3+} to Er^{3+} excites the $^4I_{15/2}$ to $^4I_{11/2}$ state followed by the redundant energy dissipated by phonons. As a consequence, Er^{3+} relaxes nonradiatively to the lower $^4I_{13/2}$ state and then suffers a second energy transfer process to $^4F_{9/2}$ state. The red emission is associated with the radiative transition from $^4F_{9/2}$ state to ground state. In addition, another energy transfer from $^4I_{11/2}$ to $^4F_{7/2}$ state results in $^2H_{11/2}/{}^4S_{3/2}$ to the ground state with the green emissions centered at

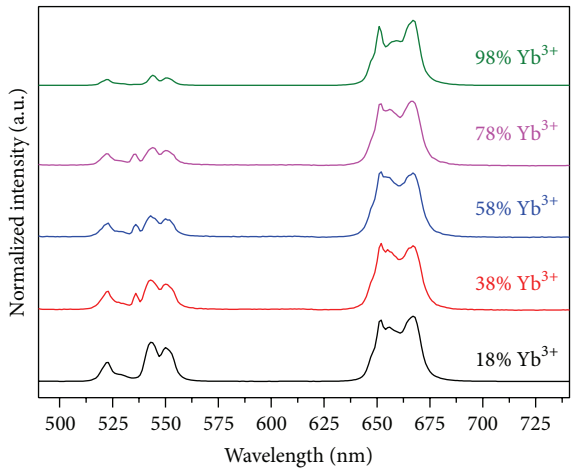

Figure 3: UC emission spectra of $KGdF_4$:x%Yb^{3+}/2%Er^{3+} (x = 18, 38, 58, 78, and 98) UCNPs.

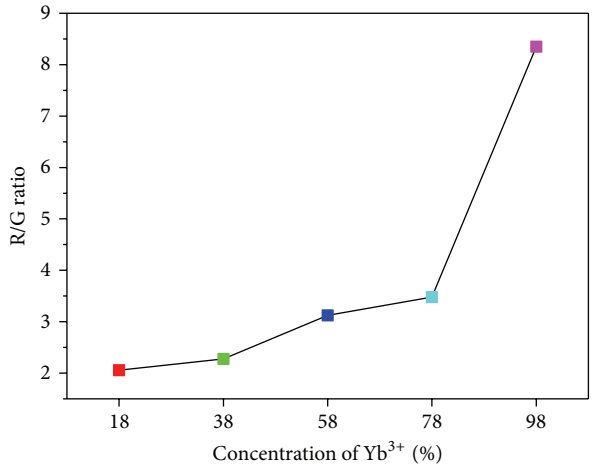

Figure 4: The variation of R/G ratio of $KGdF_4$:Yb^{3+}/Er^{3+} UCNPs as a function of Yb^{3+} concentration.

523 and 543 nm, respectively, followed by the corresponding nonradiative relaxations. However, the increase of the doped Yb^{3+} concentration into the host results in the inhibition of green emission and the enhancement of R/G ratio when ranging Yb^{3+} concentration from 18% to 98%. This is due to the decrease in average distance between Yb^{3+} and Er^{3+} with the increase in number of Yb^{3+} per Er^{3+}, which can increase the energy transfer efficiency between Yb^{3+} and Er^{3+}. However, the cross relaxation process $^4F_{7/2}$ (Er^{3+}) + $^2F_{7/2}$ (Yb^{3+}) → $^4I_{11/2}$ (Er^{3+}) + $^2F_{5/2}$ (Yb^{3+}) from Er^{3+} to Yb^{3+} is favoured at the same time, which results in the decrease of $^4F_{7/2}$ (Er^{3+}) population and green emissions [20]. As a consequence, through energy transfer process $^2F_{5/2}$ (Yb^{3+}) + $^4I_{13/2}$ (Er^{3+}) → $^2F_{7/2}$ (Yb^{3+}) + $^4F_{9/2}$ (Er^{3+}), the excited Yb^{3+} can transfer its energy to Er^{3+}, which contributes to the more population of Er^{3+} at $^4F_{9/2}$ state and results in the enhancement of red emission.

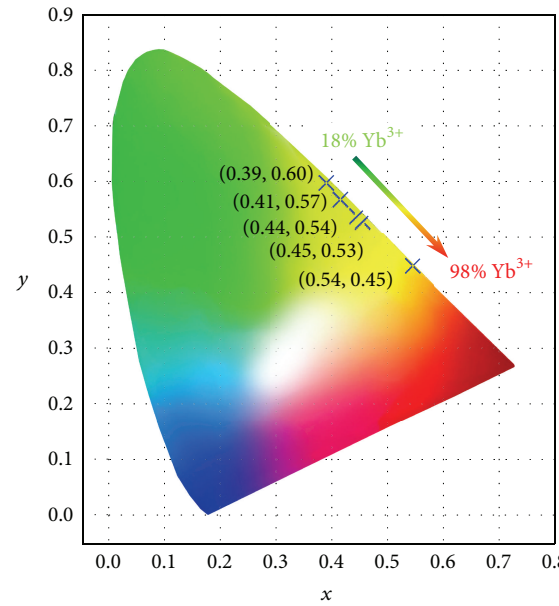

Figure 5: The CIE-1931 chromaticity diagram and calculated chromaticity coordinates of these UCNPs.

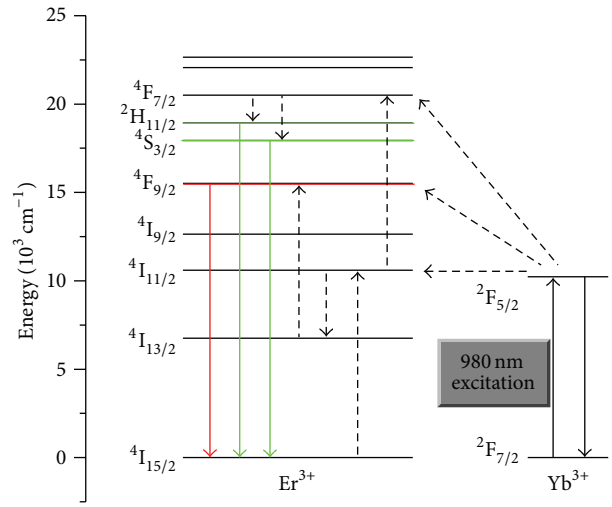

Figure 6: Schematic energy level of Yb^{3+} and Er^{3+} and their proposed energy transfer mechanisms in $KGdF_4$ UCNPs.

4. Conclusions

In conclusion, $KGdF_4$:x%Yb^{3+}/2%Er^{3+} (x = 18, 38, 58, 78, and 98) UCNPs were fabricated via a one-pot hydrothermal method using PEG as capping ligands. All these PEGylated UCNPs were cubic phase and uniformed nanoparticle shape. These UCNPs realized yellow to red color emission by tuning the Yb^{3+} concentration from 18% to 98%, as well as the R/G ratio enhancement from 2.05 to 8.35. The multicolor emission and enhanced R/G ratio revealed that these PEGylated $KGdF_4$:Yb^{3+}/Er^{3+} UCNPs can act as nanophosphors and expand their application on lighting devices, anticounterfeit technology, and even bioimaging field.

Conflict of Interests

The authors do not have any conflict of interests in their submitted paper.

Acknowledgment

This work was supported by the General Project of Hunan Provincial Education Department (11C1130).

References

[1] L. Cheng, C. Wang, L. Feng, K. Yang, and Z. Liu, "Functional nanomaterials for phototherapies of cancer," *Chemical Reviews*, vol. 114, no. 21, pp. 10869–10939, 2014.

[2] Z. Yi, S. Zeng, W. Lu et al., "Synergistic dual-modality *in vivo* upconversion luminescence/X-ray imaging and tracking of amine-functionalized $NaYbF_4$:Er nanoprobes," *ACS Applied Materials and Interfaces*, vol. 6, no. 6, pp. 3839–3846, 2014.

[3] F. Wang, R. R. Deng, J. Wang et al., "Tuning upconversion through energy migration in core-shell nanoparticles," *Nature Materials*, vol. 10, no. 12, pp. 968–973, 2011.

[4] J. Zhou, Z. Liu, and F. Y. Li, "Upconversion nanophosphors for small-animal imaging," *Chemical Society Reviews*, vol. 41, no. 3, pp. 1323–1349, 2012.

[5] S. J. Zeng, M.-K. Tsang, C.-F. Chan, K.-L. Wong, and J. H. Hao, "PEG modified $BaGdF_5$: Yb/Er nanoprobes for multi-modal upconversion fluorescent, *in vivo* X-ray computed tomography and biomagnetic imaging," *Biomaterials*, vol. 33, no. 36, pp. 9232–9238, 2012.

[6] S. Zeng, H. Wang, W. Lu et al., "Dual-modal upconversion fluorescent/X-ray imaging using ligand-free hexagonal phase $NaLuF_4$: Gd/Yb/Er nanorods for blood vessel visualization," *Biomaterials*, vol. 35, no. 9, pp. 2934–2941, 2014.

[7] Y. Liu, K. Ai, J. Liu, Q. Yuan, Y. He, and L. Lu, "A high-performance ytterbium-based nanoparticulate contrast agent for *in vivo* X-ray computed tomography imaging," *Angewandte Chemie—International Edition*, vol. 51, no. 6, pp. 1437–1442, 2012.

[8] J. Zhou, Y. Sun, X. Du, L. Xiong, H. Hu, and F. Li, "Dual-modality *in vivo* imaging using rare-earth nanocrystals with near-infrared to near-infrared (NIR-to-NIR) upconversion luminescence and magnetic resonance properties," *Biomaterials*, vol. 31, no. 12, pp. 3287–3295, 2010.

[9] Z. G. Yi, W. Lu, H. R. Liu, and S. J. Zeng, "High quality polyacrylic acid modified multifunction luminescent nanorods for tri-modality bioimaging, in vivo long-lasting tracking and biodistribution," *Nanoscale*, vol. 7, no. 2, pp. 542–550, 2015.

[10] Z. G. Yi, W. Lu, Y. R. Xu et al., "PEGylated $NaLuF_4$: Yb/Er upconversion nanophosphors for *in vivo* synergistic fluorescence/X-ray bioimaging and long-lasting, real-time tracking," *Biomaterials*, vol. 35, no. 36, pp. 9689–9697, 2014.

[11] H. Xing, S. Zhang, W. Bu et al., "Ultrasmall $NaGdF_4$ Nanodots for efficient MR angiography and atherosclerotic plaque imaging," *Advanced Materials*, vol. 26, no. 23, pp. 3867–3872, 2014.

[12] J.-C. Boyer, F. Vetrone, L. A. Cuccia, and J. A. Capobianco, "Synthesis of colloidal upconverting $NaYF_4$ nanocrystals doped with Er^{3+}, Yb^{3+} and Tm^{3+}, Yb^{3+} via thermal decomposition of lanthanide trifluoroacetate precursors," *Journal of the American Chemical Society*, vol. 128, no. 23, pp. 7444–7445, 2006.

[13] F. Wang, Y. Han, C. S. Lim et al., "Simultaneous phase and size control of upconversion nanocrystals through lanthanide doping," *Nature*, vol. 463, no. 7284, pp. 1061–1065, 2010.

[14] G. Tian, Z. Gu, L. Zhou et al., "Mn^{2+} dopant-controlled synthesis of $NaYF_4$:Yb/Er upconversion nanoparticles for *in vivo* imaging and drug delivery," *Advanced Materials*, vol. 24, no. 9, pp. 1226–1231, 2012.

[15] S. Zeng, Z. Yi, W. Lu et al., "Simultaneous realization of phase/size manipulation, upconversion luminescence enhancement, and blood vessel imaging in multifunctional nanoprobes through transition metal Mn^{2+} doping," *Advanced Functional Materials*, vol. 24, no. 26, pp. 4051–4059, 2014.

[16] G. Y. Chen, T. Y. Ohulchanskyy, R. Kumar, H. Ågren, and P. N. Prasad, "Ultrasmall monodisperse $NaYF_4$:Yb^{3+}/Tm^{3+} nanocrystals with enhanced near-infrared to near-infrared upconversion photoluminescence," *ACS Nano*, vol. 4, no. 6, pp. 3163–3168, 2010.

[17] H.-T. Wong, M.-K. Tsang, C.-F. Chan, K.-L. Wong, B. Fei, and J. H. Hao, "*In vitro* cell imaging using multifunctional small sized $KGdF_4$:Yb^{3+},Er^{3+} upconverting nanoparticles synthesized by a one-pot solvothermal process," *Nanoscale*, vol. 5, no. 8, pp. 3465–3473, 2013.

[18] J. H. Hao, Y. Zhang, and X. H. Wei, "Electric-induced enhancement and modulation of upconversion photoluminescence in epitaxial $BaTiO_3$:Yb/Er thin films," *Angewandte Chemie—International Edition*, vol. 50, no. 30, pp. 6876–6880, 2011.

[19] S. J. Zeng, J. J. Xiao, Q. B. Yang, and J. H. Hao, "Bi-functional $NaLuF_4$:Gd^{3+}/Yb^{3+}/Tm^{3+} nanocrystals: structure controlled synthesis, near-infrared upconversion emission and tunable magnetic properties," *Journal of Materials Chemistry*, vol. 22, no. 19, pp. 9870–9874, 2012.

[20] S. H. Huang, J. Xu, Z. G. Zhang et al., "Rapid, morphologically controllable, large-scale synthesis of uniform $Y(OH)_3$ and tunable luminescent properties of Y_2O_3:Yb^{3+}/Ln^{3+} (Ln = Er, Tm and Ho)," *Journal of Materials Chemistry*, vol. 22, no. 31, pp. 16136–16144, 2012.